

Development of MnO₂/rGO Composite Electrodes for Enhanced Electrochemical Supercapacitor Performance

A. Saravanan¹, P. Arunachalam², Ganta Raghotham Reddy³ and V. Vijayan⁴

¹Department of Electronics and Communication Engineering, Jaya Engineering College, Chennai, Tamil Nadu 602024, India

²Department of Biomedical Engineering, Vel Tech Rangarajan Dr. Sagunthala R&D Institute of Science and Technology, Chennai, Tamil Nadu 600 062, India

³Department of Electronics and Communication Engineering, Kakatiya Institute of Technology and Science, Telangana 506015, India

⁴Department of Mechanical Engineering, K. Ramakrishnan College of Technology, Samayapuram, Trichy, India - 621 112

Corresponding Author Email: saravanandr2006@gmail.com

<https://doi.org/10.14447/jnmes.v27i3.a06>

Received: 20/01/2024

Accepted: 30/08/2024

Keywords:

Keywords: MnO₂, reduced graphene oxide, Capacitance, Electrochemical Supercapacitors, Annealing.

ABSTRACT

Carbon composites incorporating nanosized metal oxides could be an attractive material for electrochemical energy storage electrodes. Manganese dioxide (MnO₂)/ Reduced Graphene Oxide (rGO) composites for electrochemical supercapacitors are detailed in this article. The sonochemical approach was used to prepare MnO₂/rGO composites after a simple sol-gel process and annealing at 250°C had produced MnO₂. The composites were then combined with varying quantities of rGO. Analyzing the composite's structural and crystalline properties proved that rGO and MnO₂ were mixed. A two-electrode electrochemical setup was used to demonstrate the capacitance properties of the MnO₂/rGO composite electrode using cyclic voltammetry study. In comparison to the MnO₂ electrode by itself, the specific capacitances (Cs) measured for the MnO₂/rGO composite electrode were much greater. After 2000 cycles, the MnO₂/2rGO composite electrode maintained an outstanding cycle stability, reaching a maximum Cs value of ~343.7F/g at 15 mV/s. As a result, electrodes based on produced MnO₂/rGO composites have the potential to exhibit excellent capacitive properties.

1. INTRODUCTION

Supercapacitors differ from conventional energy storage technologies like batteries and fuel cells due to their high-power density, enormous energy storage capacity, and extended cycle life. When compared to conventional capacitors, electrochemical supercapacitors offer superior capacitance values and higher energy density per unit area[1]. Supercapacitors are categorized into two primary varieties based on their energy storage methods: pseudo-capacitors and electric double-layer capacitors (EDLCs). To expedite electrosorption, intercalation between electrodes, and redox processes, pseudocapacitors and EDLCs are currently necessary[2], [3]. Pseudo-capacitors have recently gained significant interest as a potential energy storage device, as the primary charge transfer at the electrode-electrolyte interface occurs as a result of the flow of a faradic current[4]. This process is known as electrosorption or the faradaic reaction. Electrodes in pseudo-capacitors are typically made of conjugated conducting polymers, transition metal sulfides, or transition metal oxides. When compared to the materials used alone, the combination of metal oxides and carbon-based materials shows much better charging/discharging ability, capacitance value, and cyclic stability[5], [6].

A wide variety of possible catalytic uses have been shown by aerogels because of their strong structure and high adsorption capacity[7]. Electrode materials made of manganese dioxide (MnO₂) are now the most interesting option for electrochemical energy storage systems due to its capacitive responsiveness and cycling characteristics. The comparatively high surface area, which includes a high pore volume and size, of MnO₂ has made it a highly sought-after catalyst for use in a wide range of catalytic processes[8], [9]. The electrical conductivity of MnO₂ is typically low, but it can be enhanced by combining it with carbon compounds. One of the best ways to increase the capacitance and rate capabilities of supercapacitors is to create a MnO₂ composite[10]. Electrode materials in a wide range of electrical devices often make use of graphene derivatives such as GO, rGO, etc., due to their huge specific surfaces, excellent electrical conductivity, and ease of mass manufacture[11]. rGO's hydrophilicity and presence of charged structures give it excellent dispersibility in both water and organic solvents. Also, supercapacitors can't use pure MnO₂ since the material has a high conduction resistance and a very low capacitance value[12], [13]. An appealing alternative electrode material for electrochemical supercapacitors is a combination of graphene oxide and manganese dioxide.

Due to their low electronic conductivity, prior research has shown that the specific Cs of supercapacitors based on metal oxides decreases substantially as the scan rate increases [14], [15]. Adding metal oxides to carbon-based materials makes sense since composites take advantage of both components' strengths while mitigating their weaknesses. Since the flaws of graphene and metal oxides, especially MnO₂, can be balanced out by their combination, the electrochemical performance of the two materials can be enhanced [16]. As an example, rGO-MnO₂ composites were synthesized by authors [17] using a hydrothermal approach; with a sweep rate of 0.5 Ag⁻¹, they achieved a specific capacitance of 300 F g⁻¹. Authors [18] produced MnO₂ nanotubes/rGO and showed that at a rate of 0.1 Ag⁻¹, the material had a discharge capacity of 263 mAhg⁻¹. Because of their unique physicochemical characteristics, TiO₂ particles—and MnO₂ in particular—have attracted a lot of attention. Many different things have made use of these particles: gas sensors, catalysts, support materials, pigments, and even environmental purification systems [19], [20]. It is thought that high performance electrochemical devices could benefit from electrodes made of a combination of MnO₂ and GO/rGO.

Combining rGO with MnO₂ to create an effective composite may offer a significant surface area for intercalation and deintercalation, as demonstrated in this study. Electrochemical supercapacitors made of a sol-gel synthesized MnO₂ and rGO composite have been developed utilizing an inexpensive technique. The electrochemical study shows that the constructed MnO₂/rGO composite electrode has created a channel for ions to easily go through, which could lead to a decrease in ionic resistance.

2. MATERIALS AND METHODS

MnO₂ was produced using an easy solvothermal method. A mixture of 12 g of titanium (IV) butoxide, 40 mL of acetone, and 1.08 mL of acetylacetone was stirred continuously at first. Next, 15.2 mL of acetone and 2.4 mL of water were delicately combined to create a sol that subsequently turned into a wet-gel. The new solution was gradually mixed with the old one. The gel was allowed to grow at room temperature for 24 hours before being placed in a 100 mL autoclave lined with Teflon. Then, MnO₂ was produced by programming the autoclave to run for four hours at a temperature of 140°C. The final result of the solvothermal procedure was filtered and then cooked in a prepared oven overnight at 60°C. The last step was to gather all of the ingredients and transfer them to a vial for later use.

After synthesizing a series of MnO₂/rGO nanocomposite, the process of precipitation was employed. Sonicating a mixture of 10 mL of ethanol with a specific amount of as-synthesized MnO₂ and rGO for 2 hours at room temperature is a common procedure in most experiments. Filtration was subsequently employed to obtain the MnO₂/rGO nanocomposite. After filtering, the specimen was dried in an oven at 60°C for the night. Then, it was ground with an agate mortar. Changing the rGO weight ratio allowed for the synthesis of three separate nanocomposites. Each sample is called a MnO₂/1GO, MnO₂/2rGO, or MnO₂/3GO based on the MnO₂:rGO ratio, which is 1:0.05, 1:0.1, or 1:0.15, respectively.

To test the capacitive characteristics, the produced MnO₂/rGO composites were used as an electrode. To begin, a mortar was prepared by adding a mixture of 8 parts water, 1 part super P, and 1 part PTFE to a mixture of 8 parts MnO₂/rGO composite. A homogenous slurry was then created using DI water. Isopropanol and DI water were used to clean the Ni foam after it had been acid-treated to eliminate oxide residues before the slurry was cast. After cleaning the Ni foam, the resulting slurry was applied using a glass rod in a rolling procedure. The coated Ni foam was then placed in a laboratory oven set at 80°C for 20 minutes. The two-electrode electrochemical system was tested in a 3M KOH electrolyte using cyclic voltammetry (CV) analysis with a scan rate ranging from 15 to 200 mVs⁻¹. The synthesized MnO₂/rGO served as the working electrode, while a Pt plate served as the counter electrode. The potentiostat used for the analysis was a VersaSTAT4 from AMETEK, Inc. Analysis of the CV data allowed for the estimation of the individual capacitances and other factors.

3. RESULTS AND DISCUSSION

Composites containing MnO₂ and rGO sheets exhibit the presence of MnO₂ particles, indicating that the MnO₂ has been bonded to the rGO sheets. The rGO sheets are coated with a homogeneous distribution of MnO₂ particles when the ratio of MnO₂ to GO is 1:0.1. Raising the rGO concentration results in an uneven distribution of MnO₂ particles on the surfaces of the rGO sheets. Due to the huge aggregates produced by the increased rGO concentration, the surface of the MnO₂/rGO composite is not homogeneous. Because of this, it is possible that the electrochemical process will benefit from the MnO₂/2rGO composite's homogenous particle distribution. The XRD and Raman measurements are used to assess the structural properties and crystalline phases of the produced manganese oxide and MnO₂/rGO composites. XRD patterns of different composites that were produced are shown in Figure 1a. Anatase phases are inferred to be present in the produced materials due to the diffraction peaks observed at 26.4 (101), 38.8 (004), 49 (200), 55 (105), 63.8 (204), 70.7 (220), and 76.2 (215) of MnO₂. A good index to JCPDS No.: 21-1272 is seen in the obtained diffraction patterns. The crystallite size (D) of the specimen was evaluated through the Debye-Scherrer's equation. The predicted size of the MnO₂ crystallite is 14.8 nm. A significant reduction in crystallite size has been noted with the introduction of the GO. A crystallite size of around 13.7 nm was observed in the produced MnO₂/2rGO. So, the rGO peak in MnO₂/rGO composites is seen in Figure 1a. Nevertheless, additional diffraction peaks resemble MnO₂, so validating the connection between rGO and MnO₂. An optimum combination of rGO and MnO₂ materials would be MnO₂/2rGO composite, since its rGO peak is more intense than that of other MnO₂/rGO composites. Figure 1b shows the results of using Raman spectroscopy to study the MnO₂/rGO composites' structural characteristics. The B1g, A1g, and Eg phonons are identified by the Raman bands at 435, 554, and 682 cm⁻¹ in the synthesized MnO₂, respectively. These Raman bands' presence verifies that anatase MnO₂ has formed. When it comes to MnO₂/rGO composites, you can see the Raman shift bands at 1395 and 1625 cm⁻¹, which are all characteristic of MnO₂, as well as the rGO

Raman bands [21], [22]. Additional evidence that a composite of MnO₂ and rGO has formed is the presence of rGO peaks alongside MnO₂ peaks.

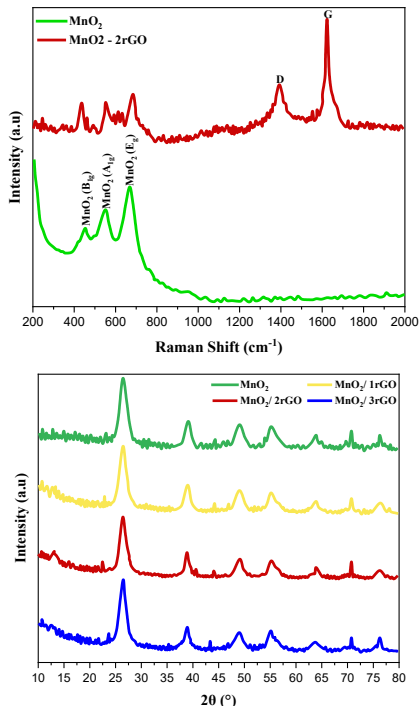
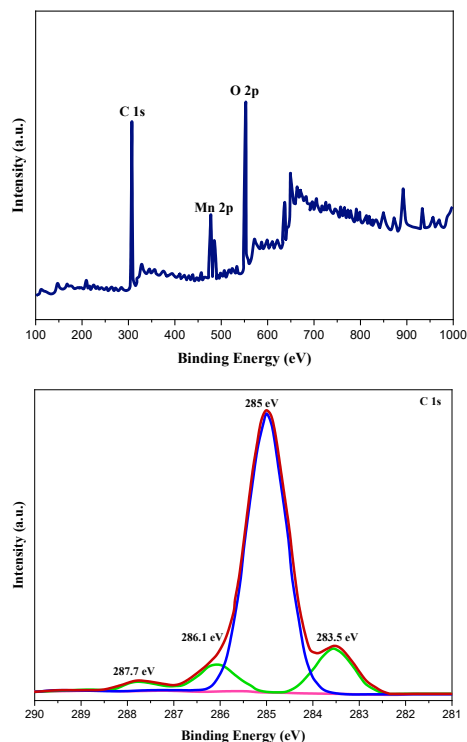


Figure 1. (a) Raman shift spectrum and (b) XRD patterns of MnO₂ and MnO₂/rGO composites.

For the MnO₂/rGO composite, the XPS results are displayed in Figure 2 a-d. Figure 2a displays the XPS survey profile, which shows the binding energies of O 1s, Mn 2p, and C 1s. According to a high-resolution Ti2p XPS spectrum (Figure 2b), the binding energies at 464.9 eV and 459.1 eV, respectively, indicate Mn 2p_{1/2} and Mn 2p_{3/2}. In addition, the reported MnO₂ materials are in good agreement with the doublet Mn 2p binding energy, which shows a peak separation of 6.1 eV[23]. Figure 2c displays the O 1s XPS spectra after deconvolution. The Ti-O bond is compatible with the main core binding energy, which is 529.9 eV[24]. Alternatively, the CO and COO groups of the rGO moiety are responsible for the two binding energies of 530.7 and 531.6 eV, respectively. Furthermore, the deconvoluted C 1s XPS spectra exhibit three distinct binding energies at 285, 286.1, and 287.7 eV, as shown in Figure 2d. These energies correspond to the sp² carbon, C O, and COO-groups in the MnO₂/rGO composite[25], [26]. The binding energy of 283.5 eV, which may be due to the M C group, indicates that MnO₂ interacts with the rGO molecule. Based on these findings, it's evident that the MnO₂/rGO composite is quite effective, thanks to the excellent interaction between the two components.

Nitrogen (N₂) adsorption-desorption isotherms were conducted to evaluate the surface areas and pore architectures of the produced MnO₂/rGO composites. The results are displayed in Fig. 3a. Figure 3a displays the isotherm for the MnO₂/2rGO composite, which has a specific surface area of 237.8 m²g⁻¹ with holes sizes 2–8 nm. Regardless of the concentration of rGO in MnO₂, the specific surface areas are decreased. In this case, the existence of micro and mesoporous surfaces in the

MnO₂/2rGO composite, along with the favorable pore size distribution, suggests that these materials could be suitable for use as electrodes in capacitive devices. By conducting CV measurements in a 3 M KOH electrolyte at 298 K, the electrochemical capacitive properties of the electrochemical supercapacitors are assessed using the produced Manganese Oxide and MnO₂/rGO composite electrodes as working electrodes. The CV plots of MnO₂ (composite-1) and various MnO₂/rGO (composite-2) composite electrodes are indicated in Figure 4a. The creation of electrochemical capacitance, often derived from faradaic pseudo-capacitance, is revealed by the low redox current response of the MnO₂ electrode, which has a nonrectangular CV shape [27], [28]. The presence of rGO materials in composite-2 electrodes is indicated by a minor shift of the redox peaks towards the positive direction. The maximum redox current was observed in the composites-2 at 2rGO electrode, which indicates that this electrode is very effective when using the ideal ratio. Figure 4b displays the CV plots of the Manganese Oxide /2rGO composite electrode. To further understand the electrochemical behavior, the scan rate is different from 15 to 200 mVs⁻¹ in a 3 M KOH electrolyte. Scan rates are positively correlated with the presence of marginal negative shifting, as seen in Figure 5 b. This finding is in line with the growing electrical polarization and irreversibility [29], [30]. By taking this into account, the process of producing capacitance or pseudo-capacitance by an irreversible Faradic reaction is clarified. The fact that CV plot shapes were affected by changes in scan rates provides more evidence that MnO₂/rGO composite electrodes exhibit pseudo-capacitance behavior and electrochemical reversibility.



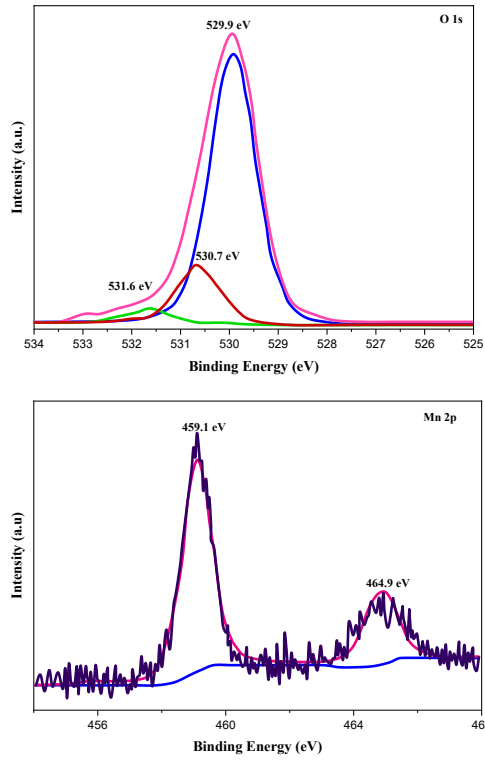


Figure 2 (a) Profiling survey, (b) C 1s, (c) O 1s, and (d) Mn 2p XPS spectrum of MnO₂/2rGO composites

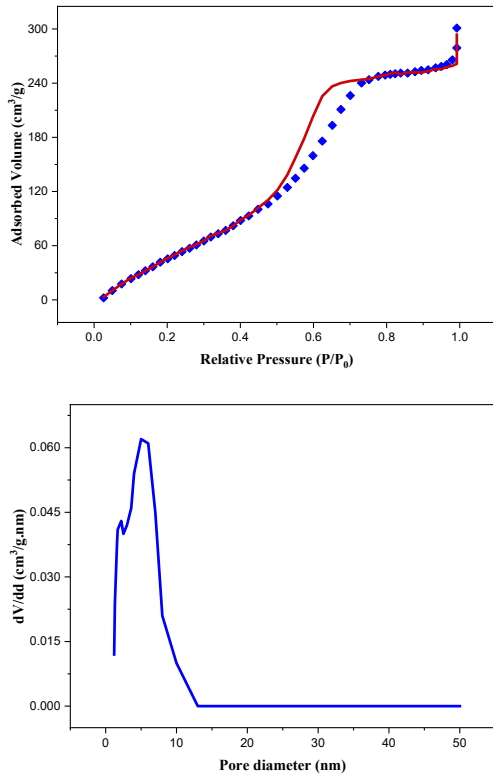


Figure 3 (a) Distribution plots for pore size and (b) N₂ adsorption-desorption isotherm for MnO₂/2rGO composites

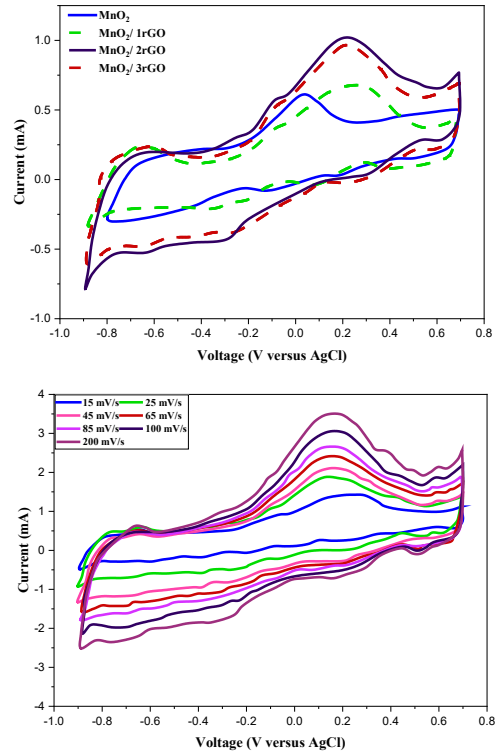


Figure 4 (b) CV plots in 3M KOH electrolyte, and (a) A series of CV plots at various scan rates for MnO₂/2rGO composite electrode

Figure 5 as shows the specific Cs of the Manganese Oxide and MnO₂/2rGO composite electrodes, which are used to evaluate the capacitive characteristics. When compared to MnO₂ and other MnO₂/rGO composite electrodes, the MnO₂/2rGO electrode shows the highest Cs at 15 mV s⁻¹ at 343.7 Fg⁻¹. The MnO₂ electrode has a very low Cs value of 76.5 Fg⁻¹, but when rGO is added to it, the Cs value increases greatly, showing that rGO is important in composites. When compared to a MnO₂ electrode, the Cs value of a composite electrode made of MnO₂ and GO is five times higher. The increase in electrical conductivity and morphological improvement caused by rGO are primarily responsible for this Cs enrichment. Thus, it may help improve the speed of ion transport and charge transfer. The retention of capacitance from the MnO₂/rGO composite electrode increases from 15 to 200 mV s⁻¹, a 33% increase over its initial value. The drop in capacitance at high scan rate can be because the material isn't as efficient. The results were confirmed by performing the galvanostatic charge discharge (GCD) test on the Manganese Oxide /rGO composite supercapacitor electrode. This study was conducted over a potential between 0 to 1.5 V using current densities ranging from 0.6 to 10 A/g. Figure 6a displays the outcomes of this analysis. A charge storage mechanism supported by pseudocapacitive nature is shown by the GCD curves, which exhibit a small divergence from the normal shape of symmetric triangles. This process probably occurs because of the electrolyte's K⁺ ions interacting with MnO₂/rGO [31], [32]. As current densities increase, the specific capacitance value decreases because the charging and discharging durations get shorter. Supercapacitors

made of MnO₂/rGO composites showed specific capacitance values of 320.6, 169.2, 95.4, and 60.7 Cg⁻¹ at 0.6, 1.2, 2.4, and 6 Ag⁻¹ current densities as shown in Figure 6 b. Since ions may only penetrate the electrode material to a certain depth, the capacitance value drops as the current densities increases. The high Cs of 320.6 Cg⁻¹ is a consequence of the prolonged discharge period and rapid ion diffusion, both of which are caused by the mixed porous structure of MnO₂/rGO composites [33]. On the other hand, increasing the concentration of rGO in composites leads to a drop in capacitance value because electrochemical processes cause the creation of many aggregates [34], [35]. The charge transfer between electrode materials and at contact interfaces is greatly hindered as a result of the ions diffusion length being prolonged. As indicates in Fig 7, the electrochemical characteristics of the MnO₂/rGO electrode composite are tested utilizing the multicycles CVs to further verify its cycling capabilities. With excellent capacitive performance, rate capability, and high cyclic ability, the composite-2 electrode retains more than 90% of the starting value even after 2000 cycles. Owing to the dual impacts of rGO on the composite, which increase electrical conductivity and surface-to-volume ratio, the composite-2 electrode in this study shows an excellent cycling capability in an alkaline electrolyte and a high Cs value. Consequently, it may promote rapid charge transfer and ion transit.

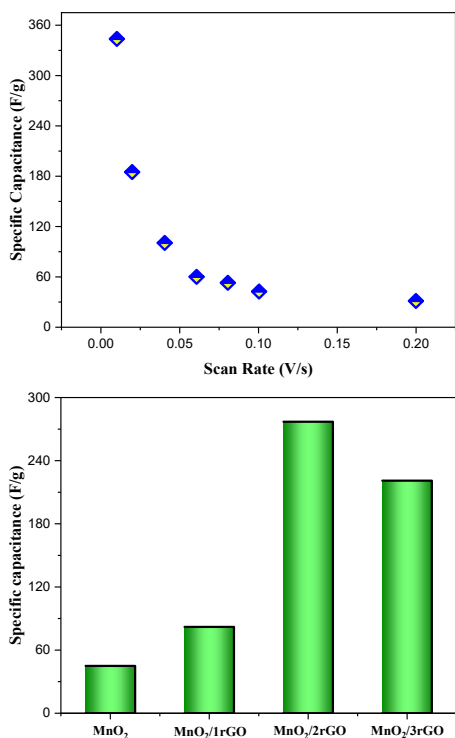


Figure 5 (a) Specific capacitances of various electrodes, and (b) evaluation of specific capacitance and scanning rate of MnO₂/2rGO composite electrode

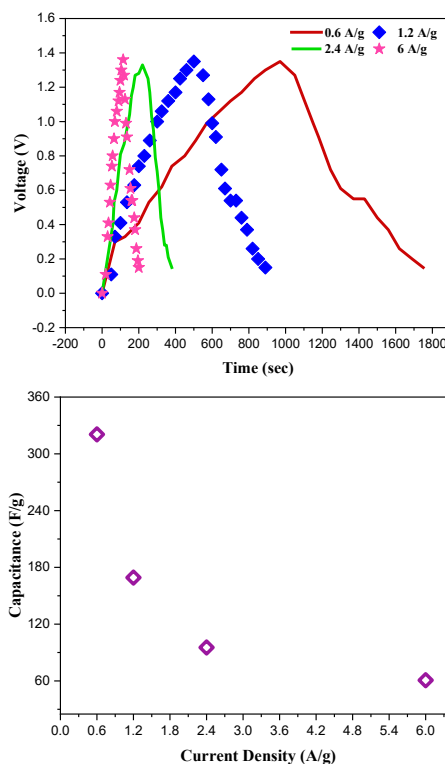


Figure 6 (a) Evaluation of Cs from GCD curvatures and current densities and (b) comparison of GCD curves with current densities for Manganese Oxide/2rGO composite electrode

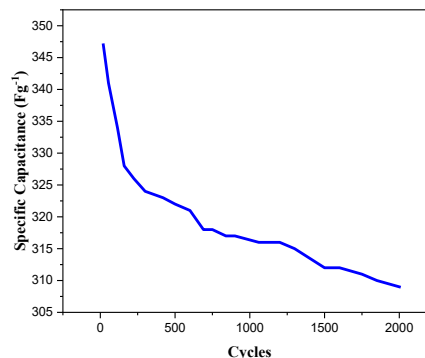


Figure 7. The MnO₂/2rGO composite electrode maintains its cycle stability even after 2000 cycles.

4. CONCLUSIONS

In electrochemical supercapacitor production, it serves as an electrode, the effective MnO₂/rGO composites are synthesized using a straightforward solution technique. Synthesizing MnO₂ using the sol-gel method is the first step in preparing MnO₂/rGO composites. Next, varying amounts of rGO are added to the produced MnO₂ using the sonochemical approach. Verification of the composite's rGO and MnO₂ integration is confirmed by several characterizations. By taking CV readings, the capacitive characteristics of MnO₂/rGO composite electrodes can be studied. One possible explanation for the higher Cs value of 343.7Fg⁻¹ at 15 mVs⁻¹ achieved by the Manganese Oxide /rGO composite electrode compared to MnO₂ and other electrodes is that the addition of rGO to the electrodes increases the electrical

conductivity and the surface-to-volume ratio. Superior cycling performance is demonstrated after 2000 cycles by the MnO₂/rGO composite electrode. Hence, the results show that electrode materials improved electrochemical behavior can be MnO₂/rGO composites with strong capacitive performance.

REFERENCES

- [1] Zaeem Ur Rehman, Mohsin Ali Raza, Uzair Naveed Chishti, Aoun Hussnain, Muhammad Faheem Maqsood, Muhammad Zahir Iqbal, Muhammad Javaid Iqbal & Umar Latif, 2023, "Role of Carbon Nanomaterials on Enhancing the Supercapacitive Performance of Manganese Oxide-Based Composite Electrodes," *Arab J Sci Eng*, vol. 48, no. 7, pp. 8371–8386. DOI:10.1007/s13369-022-06895-2
- [2] Youyi Sun, Wenhui Zhang, Diansen Li, Li Gao, Chunlin Hou, Yinghe Zhang, Yaqing Liu, 2015, "Facile synthesis of MnO₂/rGO/Ni composite foam with excellent pseudocapacitive behavior for supercapacitors," *J Alloys Compd*, vol. 649, pp. 579–584. DOI:10.1016/j.jallcom.2015.07.212
- [3] Chang, Han-Wei and Lu, Ying-Rui and Chen, Jeng-Lung and Chen, Chi-Liang and Lee, Jyh-Fu and Chen, Jin-Ming and Tsai, Yu-Chen and Yeh, Ping-Hung and Chou, Wu Ching and Dong, Chung-Li, 2016, "Electrochemical and: In situ X-ray spectroscopic studies of MnO₂/reduced graphene oxide nanocomposites as a supercapacitor," *Physical Chemistry Chemical Physics*, vol. 18, no. 28, pp. 18705–18718. DOI:10.1039/C6CP01192F
- [4] Thiagarajan, K., Jayaraman, M., Vijayan, V., Ramkumar, R. (2020). Cluster analysis of lost foam casted Al-Zn-Mg-Cu alloy with K-Mean algorithm. *Journal of New Materials for Electrochemical Systems*, Vol. 23, No. 1, pp. 45-51. DOI:10.14447/jnmes.v23i1.a09
- [5] Yiju Li, Guiling Wang, Ke Ye, Kui Cheng, Yue Pan, Peng Yan, Jinling Yin, Dianxue Cao, 2014, "Facile preparation of three-dimensional multilayer porous MnO₂/reduced graphene oxide composite and its supercapacitive performance," *J Power Sources*, vol. 271, pp. 582–588. DOI:10.1016/j.jpowsour.2014.08.048
- [6] GholamhassanImanzadeh, Zahra Zahed, Raha Hadi, Laleh Saleh Ghadimi, Sasan Shafiei, Hamid Rajabi, Erfan Ghadirzadeh, Peyman Hejazi, Nikoo Goudarzi & Mehdi Jafarian Barough, 2024 "Design and One-Pot Green Synthesis of a Three-Component 1,1'-Bi(2-Naphthol)/Reduced Graphene Oxide@MnO₂ Nanocomposite for Battery-Type Supercapacitor Applications: A Revolution in the World of Medicine," *J Electron Mater*. DOI:10.1007/s11664-024-10961-w
- [7] R. Manikandan, Prasanth Ponnusamy, S. Nanthakumar, A. Gowrishankar, V. Balambica, R. Girmurugan, S. Mayakannan, 2023, "Optimization and experimental investigation on AA6082/WC metal matrix composites by abrasive flow machining process," *Mater Today Proc*. DOI:10.1016/j.matpr.2023.03.274
- [8] S. Venkatesa Prabhu, N. R. Srinivasan, and H. Sintayehu Mekuria, Heavy metal extraction from e-waste through bioleaching: A promising ecofriendly approach. Springer International Publishing, 2021. DOI:10.1007/978-3-030-63575-6_14
- [9] S. M. Beyan, S. V Prabhu, T. A. Ambio, and C. Gomadurai, "A Statistical Modeling and Optimization for Cr(VI) Adsorption from Aqueous Media via Teff Straw-Based Activated Carbon: Isotherm, Kinetics, and Thermodynamic Studies," *Adsorption Science and Technology*, vol. 2022, 2022. DOI:10.1155/2022/7998069
- [10] Roseline, S., Paramasivam, V., Parameswaran, P., Antony, A.G. (2019). Evaluation of mechanical properties and stability of Al 6061 with addition of ZrO₂ And Al₂O₃. *Journal of New Materials for Electrochemical Systems*, Vol. 22, No. 1, pp. 21-23. DOI: 10.14447/jnmes.v22i1.a05
- [11] Sathish, T., Chandramohan, D., Vijayan, V., Sebastian, P.J. (2019). Investigation on microstructural and mechanical properties of Cu reinforced with Sic composites prepared by microwave sintering process. *Journal of New Materials for Electrochemical Systems*, Vol. 22, No. 1, pp. 5-9. DOI:10.14447/jnmes.v22i1.a02
- [12] V. M. Vimuna, B. N. Bessy Raj, S. P. Chandini Sam, and T. S. Xavier, "One-pot temperature-controlled hydrothermal synthesis of α -MnO₂ nanoparticles decorated thermally reduced graphene oxide composite as high-performance flexible aqueous symmetric supercapacitors," *Diam Relat Mater*, vol. 120, 2021. DOI:10.1016/j.diamond.2021.108707
- [13] G. P. Ojha, B. Pant, S.-J. Park, M. Park, and H.-Y. Kim, "Synthesis and characterization of reduced graphene oxide decorated with CeO₂-doped MnO₂ nanorods for supercapacitor applications," *J Colloid Interface Sci*, vol. 494, pp. 338–344, 2017. DOI:10.1016/j.jcis.2017.01.100
- [14] A. M. Gejea, S. Mayakannan, R. M. Palacios, A. A. Hamad, B. Sundaram, and W. Alghamdi, "A Novel Approach to Grover's Quantum Algorithm Simulation: Cloud-Based Parallel Computing Enhancements," in *Proceedings of the 4th International Conference on Smart Electronics and Communication, ICOSEC 2023*, 2023, pp. 1740–1745. DOI:10.1109/ICOSEC58147.2023.10276383
- [15] S. Mayakannan, M. Saravanan, R. Arunbharathi, V. P. Srinivasan, S. V Prabhu, and R. K. Maurya, *Navigating Ethical and Legal Challenges in Smart Agriculture: Insights from Farmers*. 2023. (pp.175-190) DOI:10.1201/9781003391302-10
- [16] Venkatramanan Varadharajan, Dilip Saravanan Senthilkumar, Kathiresan Senthilkumar, Venkatesa Prabhu Sundramurthy, Rahul Manikandan, Hariprasath Senthilarasan, Harish Ganesan, Indiravadanan Kesavamoorthy, Arulvel Ramasamy, 2022, "Process modeling and toxicological evaluation of adsorption of tetracycline onto the magnetized cotton dust biochar," *Journal of Water Process Engineering*, vol. 49. DOI:10.1016/j.jwpe.2022.103046
- [17] M. Ates, O. Kuzgun, M. Yildirim, and H. Ozkan, "rGO / MnO₂ / Polyterthiophene ternary composite: pore size control, electrochemical supercapacitor behavior and equivalent circuit model analysis," *Journal of Polymer Research*, vol. 27, no. 8, 2020. DOI:10.1007/s10965-020-02183-5

- [18] R. Girimurugan, C. Shilaja, A. Ranjithkumar, R. Karthikeyan, and S. Mayakannan, "Numerical Analysis of Exhaust Gases Characteristics in Three-Way Catalytic Converter Using CFD," in AIP Conference Proceedings, 2023. DOI:10.1063/5.0150561
- [19] K. Shanmuganandam, S. Thanikaikarasan, T. Ahamad, S. Ali, and V. P. Sundramurthy, "Structure, Surface Nature, Thermal Stability, and Biomass Gasification Process of NiO/SiO₂ and NiO-Pr₂O₃/SiO₂ Nanocomposites Obtained through Facile Deposition Precipitation Method," J Nanomater, vol. 2022, 2022. DOI:10.1155/2022/1479808
- [20] Vijayakumar Arun, R. Kannan, S. Ramesh, M. Vijayakumar, P. S. Raghavendran, M. Siva Ramkumar, P. Anbarasu, Venkatesa Prabhu Sundramurthy, 2022 "Review on Li-Ion Battery vs Nickel Metal Hydride Battery in EV," Advances in Materials Science and Engineering, vol. 2022. DOI:10.1155/2022/7910072
- [21] R. Rajagopal and K.-S. Ryu, "Synthesis of La and Ce Mixed MnO₂ Nanostructure/rGO Composite for Supercapacitor Applications," ChemElectroChem, vol. 5, no. 16, pp. 2218–2227, 2018. DOI:10.1002/celec.201800533
- [22] J. R. Xavier and S. P. Vinodhini, "Fabrication of reduced graphene oxide encapsulated MnO₂/MnS₂ nanocomposite for high performance electrochemical devices," Journal of Porous Materials, vol. 30, no. 6, pp. 1897–1910, 2023. DOI:10.1007/s10934-023-01473-9
- [23] B. Mu, W. Zhang, S. Shao, and A. Wang, "Glycol assisted synthesis of graphene-MnO₂-polyaniline ternary composites for high performance supercapacitor electrodes," Physical Chemistry Chemical Physics, vol. 16, no. 17, pp. 7872–7880, 2014. DOI:10.1039/c4cp00280f
- [24] C. Poochai et al., "Alpha-MnO₂ nanofibers/nitrogen and sulfur-co-doped reduced graphene oxide for 4.5 V quasi-solid state supercapacitors using ionic liquid-based polymer electrolyte," J Colloid Interface Sci, vol. 583, pp. 734–745, 2021. DOI:10.1016/j.jcis.2020.09.045
- [25] F. Mahdi, M. Javanbakht, and S. Shahrokhian, "Facile In-Situ Electrosynthesis of MnO₂/RGO Nanocomposite for Enhancing the Electrochemical Performance of Symmetric Supercapacitors," Journal of Electroanalytical Chemistry, vol. 957, 2024. DOI:10.1016/j.jelechem.2024.118099
- [26] A. Y. Faid and H. Ismail, 2019 "Ternary mixed nickel cobalt iron oxide nanorods as a high-performance asymmetric supercapacitor electrode," Mater Today Energy, vol. 13, pp. 285–292. DOI:10.1016/j.mtener.2019.06.009
- [27] F. Rahmanabadi, P. Sangpour, and A. A. Sabouri-Dodaran, "Electrochemical Deposition of MnO₂/RGO Nanocomposite Thin Film: Enhanced Supercapacitor Behavior," J Electron Mater, vol. 48, no. 9, pp. 5813–5820, 2019. DOI:10.1007/s11664-019-07361-w
- [28] A. S. Vedpathak, M. A. Desai, S. Bhagwat, and S. D. Sartale, "Green Strategy for the Synthesis of K⁺Pre-inserted MnO₂/rGO and Its Electrochemical Conversion to Na-MnO₂/rGO for High-Performance Supercapacitors," Energy and Fuels, vol. 36, no. 8, pp. 4596–4608, 2022. DOI:10.1021/acs.energyfuels.2c00381
- [29] M. Zhang, D. Yang, and J. Li, "Supercapacitor performances of MnO₂ and MnO₂/ reduced graphene oxide prepared with various electrodeposition time," Vacuum, vol. 178, 2020. DOI:10.1016/j.vacuum.2020.109455
- [30] S. Hassan, M. Suzuki, and A. A. El-Moneim, "Facile synthesis of MnO₂/graphene electrode by two-steps electrodeposition for energy storage application," Int J Electrochem Sci, vol. 9, no. 12, pp. 8340–8354, 2014. DOI:10.1016/S1452-3981(23)11051-0
- [31] G. A. M. Ali, "Recycled MnO₂ Nanoflowers and Graphene Nanosheets for Low-Cost and High Performance Asymmetric Supercapacitor," J Electron Mater, vol. 49, no. 9, pp. 5411–5421, 2020. DOI:10.1007/s11664-020-08268-7
- [32] B. G. Choi, "Development of high-performance supercapacitors based on MnO₂/functionalized graphene nanocomposites," Applied Chemistry for Engineering, vol. 27, no. 4, pp. 439–443, 2016. DOI:10.14478/acc.2016.1061
- [33] P. Y. Chan and S. R. Majid, "RGO-wrapped MnO₂ composite electrode for supercapacitor application," Solid State Ion, vol. 262, pp. 226–229, 2014. DOI:10.1016/j.ssi.2013.10.005
- [34] F. Mahdi, M. Javanbakht, and S. Shahrokhian, "In-site pulse electrodeposition of manganese dioxide/reduced graphene oxide nanocomposite for high-energy supercapacitors," J Energy Storage, vol. 46, 2022. DOI:10.1016/j.est.2021.103802
- [35] J. Kim, S. C. Byun, S. Chung, and S. Kim, "Preparation and capacitance properties of graphene based composite electrodes containing various inorganic metal oxides," Carbon Letters, vol. 25, no. 1, pp. 14–24, 2018. DOI:10.5714/CL.2018.25.014
- [36] S. Dinesh, A. Godwin Antony, S. Karuppusamy, V. Vijayan and B. Suresh Kumar, 2016. Experimental investigation and optimization of machining parameters in CNC turning operation of duplex stainless steel. Asian Journal of Research in Social Sciences and Humanities 6, pp. 179-195. DOI:10.5958/2249-7315.2016.01006.6
- [37] S. Dinesh, A. Godwin Antony, K. Rajaguru and V. Vijayan. 2016. Investigation and Prediction of material removal rate and surface roughness in CNC turning of EN24 alloy steel, Asian Journal of Research in Social Sciences and Humanities , vol 6 (8) 849–863. DOI:10.5958/2249-7315.2016.00654.7
- [38] T. Tamizharasan, N. Senthil Kumar, V. Selvkumar, S. Dinesh, 2019. Taguchi's Methodology of optimizing turning parameters over chip thickness ratio in machining PM AMMC, SN Appl. Sci. 1: 160., Springer Publishers. DOI:10.1007/s42452-019-0170-8